JOURNAL OF Materials CHEMISTRY

Layer-by-layer depositions of polyelectrolyte/CdTe nanocrystal films controlled by electric fields

Junqi Sun,[a,b,c] Mingyuan Gao,*[a,b] Min Zhu,[a] Jochen Feldmann[b] and Helmuth Möhwald[a]

[a]*Max-Planck-Institut für Kolloid- und Grenzflächenforschung, am Mühlenberg 2, 14476. Golm/Potsdam, Germany*
[b]*Photonics and Optoelectronics Group, Department of Physics and CeNS, University of Munich, Amalienstr. 54, D-80799 Munich, Germany. E-mail: gaomingyuan@hotmail.com*
[c]*Key Lab of Supramolecular Structure and Spectroscopy, Department of Chemistry, Jilin University, Changchun 130023, P. R. China*

Received 3rd December 2001, Accepted 26th March 2002
First published as an Advance Article on the web 26th April 2002

Electric fields are used to control the layer-by-layer deposition of positively charged poly(diallyldimethylammonium chloride) (PDDA) and negatively charged CdTe nanocrystals on Au substrates following the method of 'Electric Field Directed Layer-by-layer Assembly' (EFDLA) described in reference 7. Experimental results demonstrate that the depositions of PDDA and CdTe can be facilitated by maintaining the polarity of the electrode opposite to the sign of the charge of the deposited material (favorable deposition). In contrast, the deposition can also be prohibited when the polarity of the electrode is always the same as the sign of the charge of the deposited material (unfavorable deposition). Quartz crystal microbalance (QCM) results reveal that the prohibition of deposition on Au electrodes is realized by effectively blocking the adsorption of PDDA and desorbing in the meantime the previously adsorbed CdTe during the unfavorable deposition of PDDA. As a result, at most one bilayer of PDDA/CdTe can be deposited on the Au surface under unfavorable deposition at a voltage of 0.6 V. As for the favorably deposited PDDA/CdTe multilayer films, no obvious electrochemical degradation is observed with respect to CdTe nanocrystals in the film that is obtained by a series of favorable depositions of PDDA and CdTe performed alternately under 0.6 V. Atomic force microscopic measurements reveal that a six-bilayer PDDA/CdTe film obtained by favorable deposition has a relatively smooth surface with a surface roughness of 1.9 nm.

Introduction

Recently the fabrication of various lateral patterning structures has become a fascinating subject of research due to their potential applications in integrated optics, optoelectronic devices, sensors, optical memory devices, and so on.[1] Many methods such as soft lithography,[2] scanning probe lithography,[3] self-assembly/organization[4] as well as combinatorial approaches[5,6] have been developed for fabricating more miniaturized and complex patterning surfaces to meet different kinds of requirements.

Very recently, we have developed an *electric field directed layer-by-layer assembly* (EFDLA) method for producing lateral patterning structures of layer-by-layer (LbL) self-assembled films.[7] By defining the polarities on electrodes that are placed on a common substrate, selective deposition of multilayer self-assembled films directed by electric fields can then be realized.[7] Since the film deposition on each single electrode can be controlled independently, by a multi-step deposition laterally patterned structures consisting of different types of films on different electrodes can be obtained.[8]

In our previous report, the EFDLA deposition of highly fluorescent CdTe nanocrystals and PDDA [poly(diallyldimethylammonium chloride)] alternate films was performed using structured ITO (indium tin oxide) glass as substrate. The successful control over the film growth by electric fields was demonstrated by fluorescence spectroscopy and cross-sectional scanning electron microscopy.[7] In this paper, we report the EFDLA deposition of multilayer CdTe/PDDA films [(CdTe/PDDA)*n] (n = number of bilayers) on Au substrates. Quartz crystal microbalance (QCM), reflective UV-Visible spectroscopy and atomic force spectroscopy (AFM) were used to investigate the deposition process with respect to both PDDA and CdTe in the presence of electric fields as well as the surface morphologies of the resulting films.

In practice, EFDLA deposition is quite similar to the traditional LbL self-assembling process reported before[9] except that a certain dc voltage is used during the deposition process to control the movement and adsorption/desorption of charged species. For EFDLA deposition, conducting substrates (Au in this paper) not only supply electric fields but also serve as supporting substrates for the resultant films. In the simplest system, at least two electrodes are required. Here we denote the electrode on which film deposition is accelerated by an electric field as the working electrode, whereas the electrode on which the deposition is decelerated is denoted the counter electrode. Therefore, favorable deposition always takes place on the working electrode and the unfavorable deposition occurs on the counter electrode. In practice, favorable deposition is realized by setting the polarity on the working electrode opposite to the sign of the charge on the deposited material. Unfavorable deposition is realized by just the opposite way. Thus selective deposition of alternate multilayer films on the working electrode rather than on the counter electrode can be realized by enabling a series of favorable depositions to take place only on the working electrode. This requires the polarities on two electrodes to be switched back and forth each time the two electrodes are transferred from one polyelectrolyte solution to another solution of oppositely charged species.

Experimental

Cationically charged PDDA and ionically charged CdTe particles were used to construct multilayer films. The concentration of PDDA was 5×10^{-2} M (with respect to the repeat unit). Thioglycolic acid stabilized CdTe nanoparticles were synthesized according to ref. 10. The pH value and concentration of the CdTe solution were 7.8 ± 0.2 and 1.3×10^{-3} M (with respect to the concentration of Cd^{2+}), respectively. The average particle size of CdTe is 3.4 nm determined by high-resolution transmission electron microscopy.[11] By analytical ultra-centrifugation, the CdTe particles were measured in the size regime of 3.2–3.6 nm.[12] The (PDDA/CdTe)*n films were prepared by dipping the Au substrate alternately in PDDA and CdTe solutions. The deposition time was 4 min in both PDDA and CdTe solutions. A 3 min washing procedure with water and subsequent drying procedure using a N_2 stream were introduced immediately after the deposition of each single layer.

A homemade QCM was used to monitor the film growth during the EFDLA deposition of (PDDA/CdTe)*n films. 9 MHz quartz crystal resonators were adopted. A glass cap was used to cover one of the Au electrodes on the resonator. Then two such resonators were fixed at 4 mm distance with their unsealed electrodes facing each other. A dc voltage was applied between these two electrodes during the film deposition. The resulting frequency changes on both working electrode and counter electrode were recorded after the electrodes were dried in the N_2 stream. AFM measurements were performed with rectangular Au substrates that were used for the EFDLA deposition under the same conditions as for the QCM measurements. The rectangular Au substrates were made by peeling off thin Au films deposited on Si(100) wafers and therefore they had a very smooth surface. UV-Visible spectra of PDDA/CdTe films deposited on Au substrates by both EFDLA and LbL self-assembly methods were measured in reflective mode using a Cary 50 UV-Vis spectrophotometer. A freshly prepared Au substrate was used as reference.

Results and discussion

Fig. 1 shows frequency changes on both working and counter electrodes during the deposition of a (CdTe/PDDA)*n film under 0.6 V. The deposition procedure started with PDDA. It can be seen that adsorption of the first layer of PDDA on both the working and counter electrodes leads to similar frequency changes although the polarity on the counter electrode was positive, which is supposed to make the deposition of PDDA on the counter electrode unfavorable. The following deposition of the first layer of CdTe nanocrystals again gives rise to frequency decreases on both of the electrodes, but the frequency decrease on the counter electrode is smaller than that on working electrode. Hereafter, much different behaviors in frequency changes can be observed on the two electrodes. On the counter electrode the deposition of the second layer of PDDA (third layer in total) leads to stronger desorption of CdTe compared to that occurring on the working electrode. Immediately after the third layer, although each following deposition of CdTe always gives rise to a slightly different mass increment on the counter electrode, the subsequent deposition of PDDA always leads to the desorption of CdTe and brings the frequency back to the same value as obtained after the deposition of the first PDDA layer. This proves that the positive polarity not only prohibits the deposition of PDDA but also enables the PDDA to completely extract previously adsorbed CdTe from the Au counter electrode. As a result, the unwanted deposition is successfully prohibited on the counter electrode. Moreover, the large frequency decrease caused by the adsorption of CdTe on the counter electrode indicates that at least at 0.6 V the electric fields can barely prohibit the adsorption of CdTe on the PDDA covered counter electrode. In contrast to the counter electrode, the frequency changes on the working electrode are extremely regular starting from the third deposited layer. Although adsorption of PDDA can also induce the desorption of CdTe, still a net decrease of 180 ± 2.6 Hz, which corresponds to 156 ± 2.3 ng (1 Hz decrease corresponds to a mass increase of 0.87 ng), is observed after the deposition of each bilayer of PDDA/CdTe.

In order to get more information about the influence of the electric field on the film deposition, voltages of 1 V and 0 V were also used during the deposition of CdTe/PDDA multilayer films. The latter condition corresponds to the normal LbL self-assembling process. Frequency changes on the working electrode in these two cases together with that obtained under 0.6 V are given in Fig. 2. It can be seen that with the increase of the voltage the adsorbed quantities of both PDDA and CdTe on the working electrode increase. The average frequency decreases caused per dipping cycle are 47.8, 144.4 and 207.6 Hz for voltages of 0, 0.6 and 1.0 V, respectively, which correspond to 41.6, 125.6, 180.6 ng. By comparing with the free LbL deposition, it can be seen that the applied voltage greatly increases the adsorption of CdTe. Careful observations also suggest that the negative increments in frequency (positive increments in mass) caused by deposition of either PDDA or CdTe increase with the increase of applied voltage. When the voltage reaches 1.0 V, the frequency decreases all the time in the deposition process. In other words, the adsorbed mass of PDDA has compensated the desorbed mass of CdTe during the favorable deposition of PDDA. This proves that high electric fields facilitate the deposition of both PDDA and CdTe on the

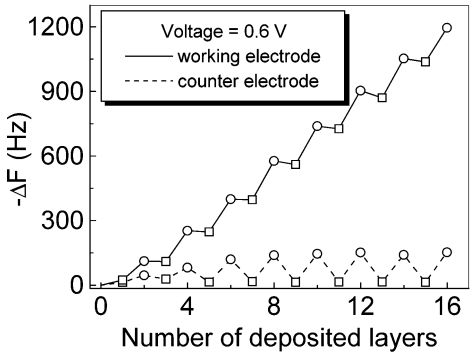

Fig. 1 Frequency decrease ($-\Delta F$) caused by deposition of (PDDA/CdTe)*n films on the QCM electrode by the EFLDA method. The working voltage is 0.6 V. Squares and circles represent frequency changes recorded after depositions of PDDA and CdTe, respectively.

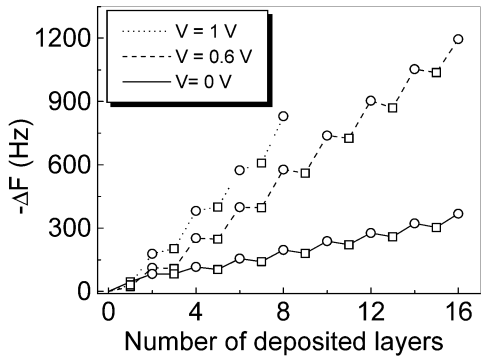

Fig. 2 Frequency decrease ($-\Delta F$) induced by the EFDLA deposition of (PDDA/CdTe)*n films on the QCM electrode at different working voltages, *i.e.*, 0 V, 0.6 and 1.0 V. The deposition under 0 V corresponds to the traditional LbL self-assembling process. Squares and circles represent frequency changes recorded after the deposition of PDDA and CdTe, respectively.

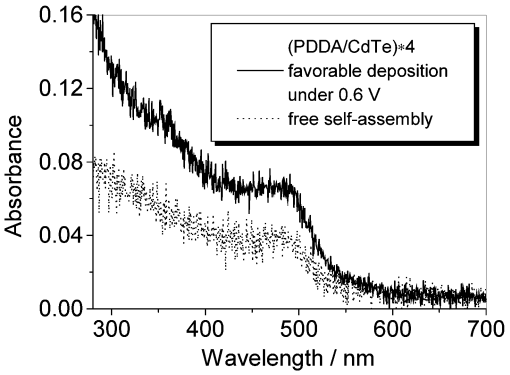

Fig. 3 Reflective UV-Visible spectra of (PDDA/CdTe)*4 films deposited on gold surfaces by (a) the LbL self-assembly method, (b) favorable EFDLA deposition with a working voltage of 0.6 V.

Au working electrode. As a result, a voltage of 1.0 V leads to the highest mass load on the working electrode within the investigated voltage range. Nonetheless, it is difficult to quantitatively differentiate mass changes solely caused by adsorptions of either PDDA or CdTe by the QCM method.

The reflective UV-Visible spectra of 4-bilayer PDDA/CdTe films deposited on Au electrodes with and without the aid of electric fields are given in Fig. 3. The latter situation again corresponds to freely self-assembling process. Except for the difference in absorbance, the absorption spectra of PDDA/CdTe films prepared by EFDLA and LbL self-assembly methods, respectively, are nearly identical in shape, which suggests that 0.6 V voltage does not cause degradation of the CdTe nanocrystals, which may be electrochemically degraded at voltage above 1 V when ITO electrodes are used instead of Au. Comparing with the freely self-assembled film, the amount of CdTe nanocrystals in the favorably deposited (PDDA/CdTe)*4 film is increased by a factor of 1.82. However, the QCM results shown in Fig. 2 give a mass increasing factor of 3.02 comparing the favorably deposited film under 0.6 V with the freely self-assembled film. This indicates that at 0.6 V the adsorption of PDDA on the working electrode is raised by a factor of 1.66 by the electric fields compared to the adsorbed amount of PDDA achieved in the freely self-assembling process. This also implies that the electric field, at least at 0.2 V mm^{-1}, has a slightly stronger influence on the deposition of the negatively charged CdTe than the positively charged PDDA on the working electrode.

The morphologies of (PDDA/CdTe)*n films prepared by the EFDLA technique and the LbL self-assembly method were investigated by AFM in tapping mode, and the AFM images of the different films are shown in Fig. 4. In each case, 6-bilayer PDDA/CdTe films were deposited on the Au surface. The freely self-assembled (PDDA/CdTe)*6 film (image c) appears very smooth with a surface roughness (square root of the standard deviation of surface fluctuation in the film normal direction) of 1.2 nm calculated from an area of 0.5 × 0.5 μm^2. The film thickness is around 15 nm measured by cross-sectional scanning electron microscopy. The surface roughness of the favorably deposited films on the working electrode is 1.9 nm when the voltage is fixed at 0.6 V (image d). In the mean time, lateral domains of about 30 nm appear in the EFDLA film. The surface roughness further increases to 2.2 nm when the applied voltage reaches 1.0 V (image e). The average size of domains also increases to about 38 nm. In contrast, the surface roughness of the bare Au substrate (image a) is only 0.7 nm. All these voltage-dependent morphologies are not surprising since both the deposition speed and the resultant film thickness increase with the increase of voltage. As a result, increased roughness and domain size are observed with the increase of applied voltage. It has already been proven by cross-sectional

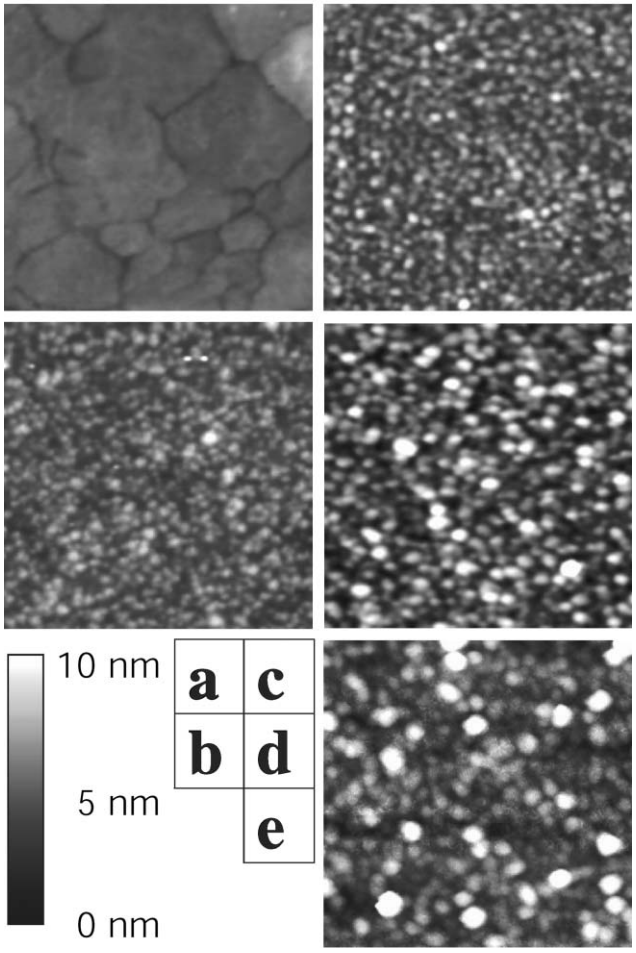

Fig. 4 AFM images: a, bare Au electrode; b, (PDDA/CdTe)*6 film on the counter electrode, $V = 0.6$ V; c, d, and e, (PDDA/CdTe)*6 films on the working electrode, $V = 0$, 0.6 V and 1.0 V.

scanning microscopy that a dense film, rather than isolated domains, is formed by favorable deposition of PDDA/CdTe films on an ITO electrode. The film thickness achieved at 1.4 V on ITO is increased by a factor of 1.4 in comparison with that of a freely self-assembled PDDA/CdTe film.[7] The AFM measurements further show that the surface of the counter Au electrode used in the EFDLA deposition at 0.6 V (image b) is rather similar to that of the working electrode. This is because the deposition of 6-bilayer PDDA/CdTe films always ended up with the CdTe layer. Therefore the counter electrode is at least covered by 1-bilayer of PDDA/CdTe as proved by the QCM measurements in Fig. 1. The surface roughness is determined to be 1.1 nm. The counter Au electrode used at 1.0 V (image not shown) appears different from that used under 0.6 V. It contains features of both the fresh Au electrode and the 0.6 V counter electrode. This indicates that a high voltage may favor the desorption of both PDDA and CdTe on the surface of the counter electrode.

In conclusion, the deposition of both PDDA and CdTe on the working electrode can be facilitated by electric fields, whereas the deposition of PDDA and CdTe on the counter electrode are prohibited by effectively blocking the adsorption of PDDA and in the mean time desorbing the previously adsorbed CdTe. QCM results demonstrate that deposition of PDDA and CdTe on the Au surface can be completely prohibited at 0.6 V. Most importantly, the reflective UV-Visible spectroscopy results prove that no degradation occurs with CdTe deposited on the working electrode. This will enable the fabrication of sophisticated lateral structures of PDDA/CdTe multilayer films on a pre-patterned Au substrate for applications in biological sensors, full color image sensors and multicolor displays.

Acknowledgement

This work has been financially supported by BMBF 03N86049. J. Q. S. gratefully thanks Dr. C. Lesser from MPIKG-Golm for her skillful assistance in QCM measurements.

References

1 Y. N. Xia, J. A. Rogers, K. E. Paul and G. M. Whitesides, *Chem. Rev.*, 1999, **99**, 1823.
2 Y. N. Xia and G. M. Whitesides, *Angew. Chem., Int. Ed.*, 1998, **37**, 550.
3 (*a*) J. A. Dagata, *Science*, 1995, **270**, 1625; (*b*) A. J. Bard, G. Denault, C. Lee, D. Mandler and D. O. Wipf, *Acc. Chem. Res.*, 1990, **23**, 357.
4 (*a*) S. I. Stupp, V. LeBonheur, K. Walker, L. S. Li, K. E. Huggins, M. Keser and A. Amstutz, *Science*, 1997, **276**, 384; (*b*) S. Gao, B. Zou, L. F. Chi, H. Fuchs, J. Q. Sun, X. Zhang and J. C. Shen, *Chem. Commun.*, 2000, 1273; (*c*) P. Qian, H. Nanjo, T. Yokoyama, T. M. Suzuki, K. Akasaka and H. Orhui, *Chem. Commun.*, 2000, 2021.
5 (*a*) X. P. Jiang and P. T. Hammond, *Langmuir*, 2000, **16**, 8501; (*b*) X. P. Jiang, S. L. Clark and P. T. Hammond, *Adv. Mater.*, 2001, **13**, 1669; (*c*) C. C. Chen, C. P. Yet, H. N. Wang and C. Y. Chao, *Langmuir*, 1999, **15**, 6845.
6 (*a*) T. Vossmeyer, S. Jia, E. Delonno, M. R. Diehl, S. H. Kim, X. Peng, A. P. Alivisatos and J. R. Heath, *J. Appl. Phys.*, 1998, **84**, 3664; (*b*) T. Vossmeyer, S. Jia, E. Delonno and J. R. Heath, *Angew. Chem., Int. Ed. Engl.*, 1997, **36**, 1080.
7 J. Q. Sun, M. Y. Gao and J. Feldmann, *J. Nanosci. Nanotechnol.*, 2001, **1**(2), 133.
8 M. Y. Gao, J. Q. Sun, E. Dulkeith, N. Gaponik, U. Lemmer and J. Feldmann, *Langmuir*, 2002, in press.
9 G. Decher, *Science*, 1997, **277**, 1232 and references therein.
10 M. Y. Gao, S. Kirstein, H. Möhwald, A. L. Rogach, A. Kornowski, A. Eychmüller and H. Weller, *J. Phys. Chem. B*, 1998, **102**, 8360.
11 A. L. Rogach, A. Eychmüller, J. Rockenberger, A. Kornowski, H. Weller, H. Tröger, M. Y. Gao, M. T. Harrison, S. V. Kershaw and M. G. Burt, *Mater. Res. Soc. Symp. Proc.*, 1999, **536**, 365.
12 C. Lesser, Ph.D thesis, Max-Planck-Institute of Colloids and Interfaces, 2001.